

DiffH₂O: Diffusion-Based Synthesis of Hand-Object Interactions from Textual Descriptions

SAMMY CHRISTEN, Meta and ETH Zurich, Switzerland
 SHREYAS HAMPALI, Meta, Switzerland
 FADIME SENER, Meta, Switzerland
 EDOARDO REMELLI, Meta, Switzerland
 TOMÁŠ HODANĚ, Meta, Switzerland
 ERIC SAUSER, Meta, Switzerland
 SHUGAO MA, Meta, USA
 BUĞRA TEKIN, Meta, Switzerland

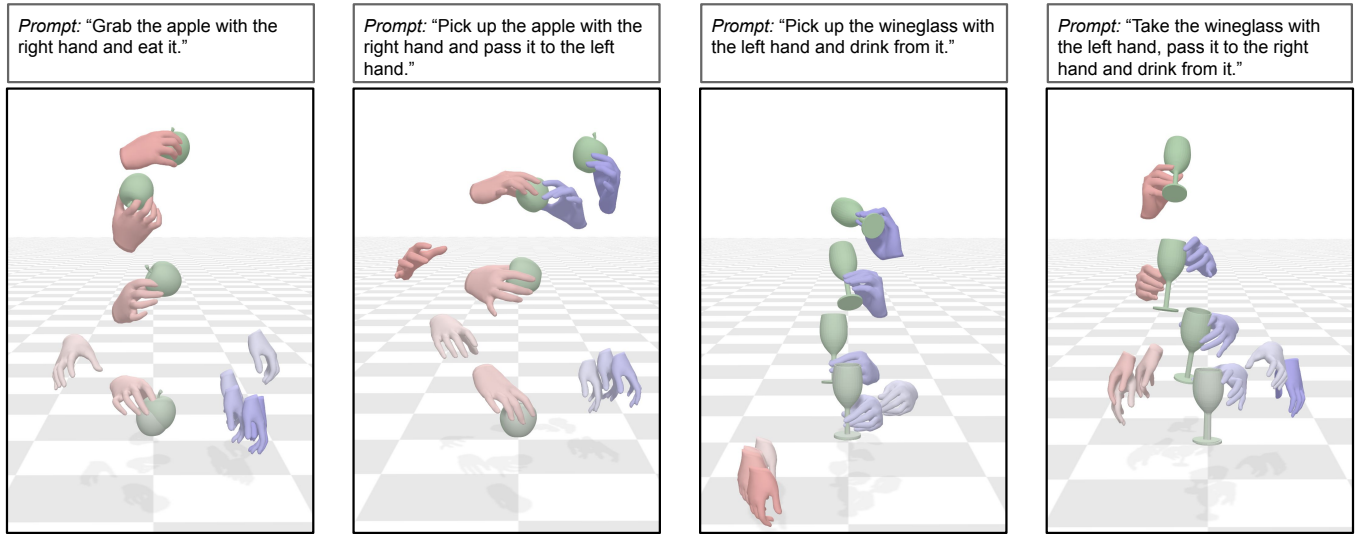


Fig. 1. We introduce DiffH₂O, a diffusion-based framework to synthesize dexterous hand-object interactions. DiffH₂O generates realistic hand-object motion from natural language, generalizes to unseen objects at test time and enables fine-grained control over the motion with detailed textual descriptions. Time is visualized with a color code where lighter shades denote the past. Best seen in the supplemental video.

Generating natural hand-object interactions in 3D is challenging as the resulting hand and object motions are expected to be physically plausible and semantically meaningful. Furthermore, generalization to unseen objects is hindered by the limited scale of available hand-object interaction datasets. We propose DiffH₂O, a novel method to synthesize realistic, one or two-handed object interactions from provided text prompts and geometry of the object. The method introduces three techniques that enable effective learning from limited data. First, we decompose the task into a grasping stage and a text-based interaction stage and use separate diffusion models for each. In the grasping stage, the model only generates hand motions, whereas in the interaction phase both hand and object poses are synthesized. Second, we propose a compact representation that tightly couples hand and object poses. Third, we propose two different guidance schemes to allow more control of the generated motions: grasp guidance and detailed textual guidance. Grasp guidance takes a single target grasping pose and guides the diffusion model to reach this grasp at the end of the grasping stage, which provides control over the grasping pose. Given a grasping motion from this stage, multiple different actions can be prompted in the interaction

phase. For textual guidance, we contribute comprehensive text descriptions to the GRAB dataset and show that they enable our method to have more fine-grained control over hand-object interactions. Our quantitative and qualitative evaluation demonstrates that the proposed method outperforms baseline methods and leads to natural hand-object motions. Moreover, we demonstrate the practicality of our framework by utilizing a hand pose estimate from an off-the-shelf pose estimator for guidance, and then sampling multiple different actions in the interaction stage. The project page along with videos can be found at <https://diffh2o.github.io/>

1 INTRODUCTION

Modeling and understanding hand-object interactions is an important and crucial task to empower machines to interact with and assist humans. Being able to seamlessly generate hand-object motions holds the promise to enable synthetic data generation [Leonardi et al. 2023], assist robots in training human-robot interactions in simulation, or enhance realism in virtual manipulation experiences. For example, in virtual reality (VR), hand interactions still often rely on heuristics and controllers that simply attach objects to the hand

according to pre-defined grasps. Being able to faithfully produce object manipulation based on an input signal such as text or a few past frames of hand and object poses could largely increase the immersiveness of such interactions.

Generating realistic hand-object interactions in 3D is challenging as the resulting motions are required to be plausible in several different aspects. First, the motions must be plausible in terms of *geometry*, such hand and object intersections are minimized and the grasp appears stable. Second, the motions must be plausible in terms of *semantics*, such as the hands respect natural object affordances (e.g., a cup is grasped by its handle and not flipped upside down). Third, the motions must be plausible in terms of *time*, such as the hand and object motions are synchronized and the dynamics appear natural. Another challenge in generating hand-object interactions comes from the limited scale of existing hand-object datasets, which are around 10x smaller than human motion datasets [Mahmood et al. 2019] and 1000x smaller than image datasets [Deng et al. 2009].

Several recent works have successfully leveraged diffusion models for full-body human motion generation but either neglect objects [Karunratanakul et al. 2023; Tevet et al. 2023] or focus only on coarse motion of larger objects (e.g., a chair) without finger predictions [Xu et al. 2023]. Another method, IMoS [Ghosh et al. 2023], can generate hand-object interactions with smaller objects (e.g., a cup or stapler) by first optimizing for upper body motions and then optimizing for object poses in a post-processing step. However, IMoS assumes that the object is in hand from the beginning, can handle only objects seen during training, and, as shown in our qualitative evaluation, the optimization often yields artifacts (e.g., hand-object interpenetration or non-plausible contact points). In this paper, we aim to learn a model that can *generate natural, fine-grained hand-object interactions and generalize to objects unseen during training*.

Towards this goal, we contribute a novel diffusion-based framework, DiffH₂O, that can generate hand-object interactions based on provided text prompts and geometry of the object. We propose several techniques to deal with the challenges of data scarcity and object generalization. **Decoupling Grasping and Interaction:** Hand-object interactions can be invariably split into a grasping phase where the hand(s) approaches the static object for grasping, and an interaction phase where the object is manipulated based on an action intent. For example, drinking from a cup can be performed with multiple grasps, and given a grasp, multiple actions are possible. We use this simple observation to obtain a grasping and an interaction diffusion model, and introduce an inpainting technique called subsequence guidance to allow continuity between the two outputs. Different from previous diffusion frameworks that employ coarse-to-fine (2D trajectory-to-full motion) two-stage generation [Karunratanakul et al. 2023], we split the task temporally. **Pose Representation:** We introduce a compact representation that models hands in parametric space. To couple the hands to the object, we represent the global hand positions relative to the normalized object pose at the initial frame and further include distance information between the 3D hand joints and the object surface. Unlike previous representations utilized in human motion diffusion [Tevet et al. 2023] and hand-object interaction [Christen et al. 2022], we find a non-redundant representation directly in parametric space to

perform best. **Controllability:** We provide two ways to add more control to our diffusion models’ output. First, we propose control through fine-grained textual descriptions. To this end, we contribute textual descriptions to the GRAB dataset and show that they enable more robustness to unseen test prompts and increase controllability, e.g., by allowing to define the interacting hand and the action to perform through the input prompts. Second, in grasp guidance, we leverage a single grasp reference which connects the grasping and interaction phase and use it to guide our two diffusion models at inference time. This grasp pose can either be obtained from motion capture or from an image-based pose estimator [Pavlakos et al. 2023] as we show in our experiments Section 5.8.

To demonstrate the effectiveness of our approach, we run perceptual studies and experiments on the GRAB dataset [Taheri et al. 2020]. We first compare against IMoS [Ghosh et al. 2023]. Our results indicate that our method generates better results across a variety of physics-based and motion metrics. To justify our technical contributions, we compare our final model against human-body diffusion baselines by adapting these methods to hand-object interactions. We show that we generate motions of higher quality while enabling more control of the outputs. Furthermore, we demonstrate that detailed textual descriptions increase robustness to unseen texts and offer better control of the diffusion model than training with heuristics-generated text descriptions. Decoupling and grasp-guidance brings high practical value to DiffH₂O. We show this with the first application of using an image-based pose/shape estimator [Pavlakos et al. 2023] to guide the diffusion to the grasp, and thereafter sampling multiple different actions through text. We prove the utility of our method by largely outperforming the state-of-the-art on a standard benchmark and in perceptual studies.

Our contributions can be summarized as follows:

- To the best of our knowledge, DiffH₂O is the first method that synthesizes hand-object interactions on unseen objects from textual descriptions, unlike previous generative models for human-body motion and seen-object HOI synthesis.
- We propose a two-stage diffusion process that splits generation into grasping and action-based interaction.
- To increase the controllability of outputs and improve generalization to unseen objects, we propose grasp guidance and subsequence guidance that can be applied at inference time to the diffusion process.
- We contribute detailed textual annotations to the GRAB dataset along with experiments showing that these textual descriptions increase robustness and enable fine-grained control of the model output.

Code and data will be made public upon acceptance.

2 RELATED WORK

2.1 Hand-Object Synthesis

Recent efforts in interaction synthesis have largely been driven by the surge of high-quality human-object interaction datasets [Brahmbhatt et al. 2019, 2020; Chao et al. 2021; Fan et al. 2023; Hampali et al. 2020; Kwon et al. 2021; Liu et al. 2022; Taheri et al. 2020]. Some studies focus on generating coarse full-body object interactions [Hassan et al. 2023; Lee and Joo 2023; Luo et al. 2021;

Wang et al. 2021; Zhang et al. 2022a], such as carrying or moving around boxes. FLEX [Tendulkar et al. 2023] trains a hand and body pose prior and later optimizes the priors to achieve diverse, static full-body grasps. GOAL [Taheri et al. 2022] and SAGA [Wu et al. 2022] use CVAEs to generate approaching motions for full-body grasps, whereas TOHO [Li et al. 2024] models both approaching and manipulation tasks via neural implicit representations. Similarly, Braun et al. [2024] model the full range of motion, leveraging physics simulation and reinforcement learning. In contrast to these works, we focus on fine-grained hand-object interactions and generalization to unseen objects. Furthermore, we leverage language prompts as input to generate interaction sequences. Among methods that model full-body object interaction, closest to our work is IMoS [Ghosh et al. 2023], a two-stage method to generate hand-object interactions on seen objects based on language commands. Starting from a grasping state, they first generate body motions and then optimize for object trajectories using a heuristics-based optimization to model hand-object interactions. By contrast, our model directly predicts the hand and object poses, models both approaching and manipulation phases, and generalizes to unseen objects.

Another line of research focuses on generation of hand-object interaction sequences in isolation from full-body due to wide applications in VR and the need for a dedicated model for fine-grained details of finger motion. One prominent solution is to turn to physical simulation and reinforcement learning [Christen et al. 2022; Garcia-Hernando et al. 2020; Mandikal and Grauman 2021; Qin et al. 2021; Rajeswaran et al. 2018]. A number of studies propose to learn dexterous manipulation tasks from full human demonstration data either collected via teleoperation [Rajeswaran et al. 2018] or from videos [Garcia-Hernando et al. 2020; Qin et al. 2021]. Mandikal and Grauman [2021] propose a reward function that incentivizes dexterous robotic hand policies to grasp in the affordance region of objects. She et al. [2022] propose a new dynamic state representation to generate dexterous grasps. D-Grasp [Christen et al. 2022] leverages reinforcement learning and physics simulation to generate diverse hand-object interactions from sparse reference inputs. ArtiGrasp [Zhang et al. 2024] extends this to two-handed grasps and generates articulated object motions.

To model hand-object interaction sequences, another solution is to rely on purely data-driven frameworks. For example, [Anonymous 2023; Zhou et al. 2022] propose methods that enable denoising hand-poses from noisy sequences of hand-object poses. Ye and Liu [2012] predict the local hand pose given full body and object motion. Similarly, ManipNet [Zhang et al. 2021] predicts local hand poses for two-handed interactions based on wrist-object trajectories. Given object motion of articulated objects, CAMS [Zheng et al. 2023] predicts one-handed poses that align with the object motion, whereas Chen et al. [2023b] focus on grasping objects using dexterity in the environment. All these works either assume a hand-object trajectory, focus only on one hand, ignore semantic action information, or do not generalize well to unseen objects. In contrast, we propose a framework that allows the synthesis of two-handed object interactions from text as well as generalization to unseen objects.

2.2 Diffusion for Motion Synthesis

Diffusion models [Sohl-Dickstein et al. 2015] have gained popularity in many domains, such as image generation [Ho et al. 2020], video generation [Yang et al. 2023], audio synthesis [Kong et al. 2021] or hand reconstruction [Ye et al. 2023a,b]. More recently, diffusion models have also been adapted to human motion synthesis [Tevet et al. 2023; Zhang et al. 2022b]. Various improvements have been proposed, such as integrating physics [Yuan et al. 2023], scene-awareness [Huang et al. 2023], increasing efficiency by diffusing in a pre-trained latent space [Chen et al. 2023a], or the composition of multiple actions [Athanasios et al. 2022]. To enable more controllability during motion synthesis, a two-stage framework, GMD, that guides the diffusion model towards target objectives at inference time is proposed in Karunratanakul et al. [2023]. However, GMD contains design choices specific to human motion generation, by first generating a 2D root trajectory over the whole sequence, and then generating corresponding full-body poses, which is not directly transferable to HOI. While these works focus on human motion in isolation from objects, InterDiff [Xu et al. 2023] generates human-object interactions via diffusion models. Their work is improved upon by recent concurrent works [Diller and Dai 2023; Li et al. 2023; Peng et al. 2023] that leverage contact-based predictions in combination with inference time-guidance to improve the interaction quality. However, these works focus on full-body motions and neglect intricate hand-object interactions. In contrast, we focus on the detailed interactions of fingers and objects. Most similar to ours, the concurrent work MACS [Shimada et al. 2023] proposes a diffusion model for hand-object motion synthesis. Their focus is on synthesizing interactions for a single object with varying mass, while our focus is on generalization to unseen shapes and interaction synthesis conditioned on text.

3 DENOISING DIFFUSION PROBABILISTIC MODELS

Denoising Diffusion Probabilistic Models (DDPM) [Ho et al. 2020; Sohl-Dickstein et al. 2015] aim to model the probability distribution of a given dataset and can model complex distributions of images [Rombach et al. 2022], videos [Ho et al. 2022] or time-series data such as motion sequences [Tevet et al. 2023].

The diffusion model involves a forward process, which is a Markov chain and consists of sequentially adding Gaussian noise to the data $\mathbf{x}_0 \sim q(\mathbf{x}_0)$. Each step in the forward noising process results in a distribution, $q(\mathbf{x}_t | \mathbf{x}_{t-1}) = \mathcal{N}(\sqrt{\beta_t} \mathbf{x}_{t-1}, (1 - \beta_t) \mathbf{I})$, where $\beta_t \in (0, 1)$ is a hyper-parameter and $t \in [1, T]$, where T is the final number of steps. Alternatively, \mathbf{x}_t can be expressed in terms of \mathbf{x}_0 as

$$\mathbf{x}_t = \sqrt{\bar{\alpha}_t} \mathbf{x}_0 + \sqrt{1 - \bar{\alpha}_t} \epsilon, \quad (1)$$

where, $\bar{\alpha}_t = \prod_{s=1}^t (1 - \beta_s)$.

The reverse process, also called the denoising process is another Markov chain with learned Gaussian transitions starting at $\mathbf{x}_T \sim \mathcal{N}(0, \mathbf{I})$. The denoised distribution at step t is given by, $p_\theta(\mathbf{x}_{t-1} | \mathbf{x}_t) = \mathcal{N}(\mu_\theta(\mathbf{x}_t, t), \sigma_t \mathbf{I})$, where θ are the model parameters to be learnt, $\mu_\theta(\cdot)$ is the mean, and σ_t is the variance. The process of data generation involves sequentially drawing samples from this distribution. The variance σ_t is usually set to $\hat{\beta}_t$ and $\mu_\theta(\mathbf{x}_t, t)$ which is implemented using an auto-encoder trained to match the mean of

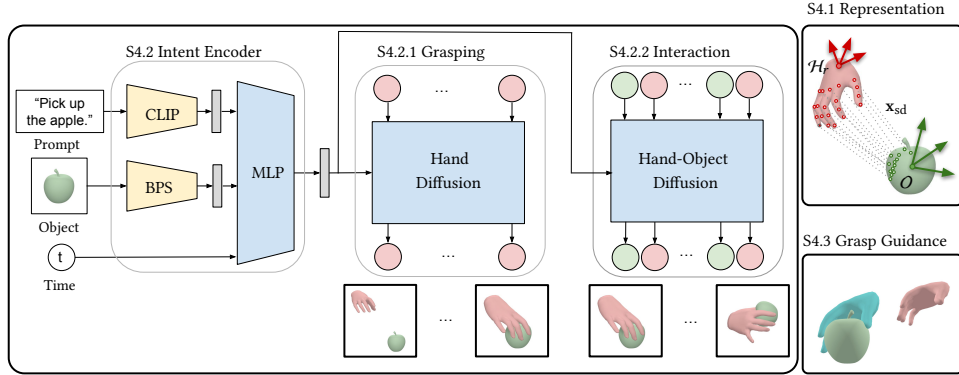


Fig. 2. **Overview of our DiffH₂O approach** Our goal is to generate realistic and controllable hand-object interactions based on user intent. We couple hands and objects by representing hand pose in object relative coordinates, and introducing variables that explicitly model hand-object distance (Sec. 4.1). We observe that objects are static until they have been grasped, and propose to inject inductive bias into our pipeline by decoupling grasping and interaction stages and modelling them with two different diffusion processes (Sec. 4.2). Finally, we make use of grasp guidance to ensure a smooth transition between these two stages (Sec. 4.2.3). We further show fine-grained controllability of our synthesis results through detailed textual descriptions (Sec. 4.4).

forward process posterior $q(x_{t-1}|x_t, x_0)$ which is another Gaussian represented as, $\mathcal{N}(\tilde{\mu}_t(\mathbf{x}_t, \mathbf{x}_0), \tilde{\beta}_t \mathbf{I})$, where

$$\tilde{\mu}_t(\mathbf{x}_t, \mathbf{x}_0) = \frac{\sqrt{\alpha_t} \beta_t}{1 - \alpha_t} \mathbf{x}_0 + \frac{\sqrt{1 - \beta_t} (1 - \alpha_{t-1})}{1 - \alpha_t} \mathbf{x}_t \quad (2)$$

and $\tilde{\beta}_t = \frac{1 - \alpha_{t-1}}{1 - \alpha_t} \beta_t$.

The auto-encoder could directly estimate the mean $\tilde{\mu}_t$ or \mathbf{x}_0 in Eq. 2, or the noise ϵ which is used in the noising process of Eq. 1. When estimating the noise, the denoised mean is obtained as $\mu_\theta(\mathbf{x}_t, t) = \frac{1}{\sqrt{1 - \beta_t}} (\mathbf{x}_t - \frac{\beta_t}{\sqrt{1 - \alpha_t}} \epsilon_\theta(\mathbf{x}_t, t))$, where $\epsilon_\theta(\mathbf{x}_t, t)$ is the auto-encoder output. The auto-encoder is trained to minimize

$$\mathcal{L}_{\text{Diff}} = \mathbb{E}_{\epsilon \sim \mathcal{N}(0, \mathbf{I}), t} \text{Loss}_{ae}, \quad (3)$$

where, Loss_{ae} is either $\|\epsilon_\theta(\mathbf{x}_t, t) - \epsilon\|_2^2$, $\|\mu_\theta(\mathbf{x}_t, t) - \tilde{\mu}_t(\mathbf{x}_t, \mathbf{x}_0)\|_2^2$, or $\|\mathbf{x}_{0, \theta}(\mathbf{x}_t, t) - \mathbf{x}_0\|$.

Conditional diffusion models generate output conditioned on various kinds of input such as text [Rombach et al. 2022] and other semantic information [Zhang et al. 2023]. Such a model is obtained by providing the condition as additional input to the auto-encoder resulting in outputs $\epsilon_\theta(\mathbf{x}_t, t, \mathbf{c})$, $\mu_\theta(\mathbf{x}_t, t, \mathbf{c})$ or $\mathbf{x}_{0, \theta}(\mathbf{x}_t, t, \mathbf{c})$, where \mathbf{c} is the conditional input encoding.

3.1 Guiding the diffusion model

Diffusion models can be guided to generate outputs of the required form. Two popular methods to guide the diffusion models are classifier guidance [Dhariwal and Nichol 2021] and classifier-free guidance [Ho and Salimans 2022]. We describe here the classifier-free guidance method which is more relevant to our work and refer the reader to [Ho and Salimans 2022] for details on classifier-free guidance.

The classifier-guidance method approximates $p(\mathbf{x}_{t-1}|\mathbf{x}_t, \mathbf{c}) \propto p_\theta(\mathbf{x}_{t-1}|\mathbf{x}_t)p(\mathbf{c}|\mathbf{x}_{t-1})$, where \mathbf{c} is the guidance, by a Gaussian:

$$\mathcal{N}(\mu_\theta(\mathbf{x}_t, t) + s \tilde{\beta} \nabla_{\mathbf{x}_t} \log p(\mathbf{c}|\mathbf{x}_t), \tilde{\beta}_t \mathbf{I}). \quad (4)$$

Intuitively, the scaled gradient of the guidance signal, $\nabla_{\mathbf{x}_t} \log p(\mathbf{c}|\mathbf{x}_t)$ is used to nudge the denoised mean μ_θ to generate samples in accordance with the guidance \mathbf{c} . $\log p(\mathbf{c}|\mathbf{x}_t)$ could represent the class probability which can be implemented using a neural-net [Dhariwal

and Nichol 2021], or could represent a cost term $G(\mathbf{x}_t)$ that is optimized [Karunratanakul et al. 2023]. The classifier guidance method has the advantage that any guidance signal that is differentiable can be used to guide the diffusion and can use pre-trained diffusion models without retraining them.

4 METHOD

We focus on the task of generating a sequence of hand and object poses $\mathbf{x} = (\mathcal{H}_l, \mathcal{H}_r, \mathcal{O})$, where $(\mathcal{H}_l, \mathcal{H}_r)$ indicate a sequence of left and right hand poses, and \mathcal{O} is a sequence of object poses given some input conditioning signal \mathbf{c} , which in our case comprises a text description and the object mesh. In other words, we want to model a conditional probability distribution $p(\mathbf{x} | \mathbf{c}, G = 0)$ with a motion DDPM. The optional term $G = 0$ is a differentiable goal function that should be minimized, e.g., the distance to a target grasp. See Fig. 2 for an overview.

In Sec. 4.1, we introduce a compact representation that tightly couples the hand and object poses and helps in generating realistic hand-object interactions. We propose a two-stage generation of hand-object interactions in Sec. 4.2 and grasp guidance in Sec. 4.3. Lastly, in Sec. 4.4, we introduce our newly-collected detailed textual annotations for the GRAB dataset that enable more controlled generation of hand-object interactions.

4.1 Canonicalized Hand-Object Representation

Our proposed representation \mathbf{x} of length N contains information about both hands and an object. In particular, the object poses are defined as $\mathcal{O} = (\boldsymbol{\tau}_o, \boldsymbol{\phi}_o)$, where $\boldsymbol{\tau}_o := (\boldsymbol{\tau}_o^0, \boldsymbol{\tau}_o^1, \dots, \boldsymbol{\tau}_o^{N-1})$ is a sequence of 3D object locations, with $\boldsymbol{\tau}_o^i \in \mathbb{R}^3$, and $\boldsymbol{\phi}_o := (\boldsymbol{\phi}_o^0, \boldsymbol{\phi}_o^1, \dots, \boldsymbol{\phi}_o^{N-1})$ is a sequence of 3D object orientations, with $\boldsymbol{\phi}_o^i \in \mathbb{R}^6$ given in 6D representation [Zhou et al. 2019]. The hands are represented by: $\mathcal{H}_j = (\boldsymbol{\tau}, \boldsymbol{\phi}, \boldsymbol{\theta}, \mathbf{x}_{sd})$, $j \in \{l, r\}$, where l denotes the left and r denotes the right hand. This representation is based on the parametric MANO hand model [Romero et al. 2017]. Specifically, the global 3D positions of the hands are given by $\boldsymbol{\tau} \in \mathbb{R}^{3 \times N}$ and the global 3D orientations are represented by $\boldsymbol{\phi} \in \mathbb{R}^{6 \times N}$. To achieve more natural poses, we define the local hand pose in a PCA space of the MANO

model with the first 24 components as $\theta \in \mathbb{R}^{24}$. Lastly, $\mathbf{x}_{sd} \in \mathbb{R}^{21 \times 3}$ denotes distances between each hand joint (including the fingertips) and its closest point on the object mesh. As we show in our ablations (see Tab. 4) this representation reduces physical artifacts such as interpenetration. We first normalize the object positions to be at the origin and then adjust the hands’ positions accordingly. Hence, all position components are relative to the object origin at the initial frame. Due to the limited data, such a representation performs better than a per-frame object-relative representation [Christen et al. 2022; Zhang et al. 2024] as we show in 5.6.

4.2 Two-Stage Hand-Object Generation

We propose to split the synthesis into grasping and interaction stages to facilitate generalization to unseen objects. The grasping stage models the motion from an initial pose to an object grasp. The interaction stage performs an action-based manipulation of the object. Our two-phase approach is motivated by the fact that any hand-object interaction involves an approaching phase where one or two hands grasp a static object, followed by an intent-driven interaction with the object. By decoupling the action-based manipulation from grasping, we can leverage the entire set of motions in the dataset for training the grasping phase, irrespective of the action that is performed in the interaction phase. This insight helps counteract the limited scale of the dataset.

As shown in Fig. 2, our grasping and interaction diffusion models are conditioned on three types of inputs to encode intent, namely, 1) text prompts describing the object and the action to be carried out, 2) object mesh which provides the geometry of the object, and 3) the time step t in the denoising process. We use CLIP [Radford et al. 2021] embeddings to encode the text prompt denoted by \mathcal{T} , BPS [Prokudin et al. 2019] to encode the object mesh denoted by \mathcal{M} and an MLP to encode the time step as in previous works [Dhariwal and Nichol 2021; Karunratanakul et al. 2023]. We provide more implementation details in supplementary material and describe the grasping and interaction phases below in detail.

4.2.1 Grasping Stage. The grasping phase is defined as a sequence containing one or two hands approaching a static object from a rest pose until the object is grasped. As the object is static throughout this phase we do not predict the object motion and only model the hand pose sequence. In order to obtain the training data for this phase we use heuristics based on object poses to determine sequence boundaries from the larger action sequences and normalize the sequence lengths by interpolating or downsampling the poses. The text description in this phase is a generic sentence ("The person grasps the <object>").

We use the ϵ_θ diffusion model that directly predicts the noise (see Section 3) in classifier-free manner [Ho and Salimans 2022] which is more susceptible to inference-time guidance as shown in GMD [Karunratanakul et al. 2023]. In other words, our grasping diffusion model training loss is given by

$$\mathbb{E}_{\epsilon \sim \mathcal{N}(0,1), t} \|\epsilon_\theta(\mathbf{x}_t, \mathcal{T}, \mathcal{M}, t) - \epsilon\|_2^2, \quad (5)$$

where \mathbf{x}_t indicates the synthesized motion at diffusion step t .

4.2.2 Interaction Stage. This phase comprises the motion of both hands and the object after a grasp has been established. In this

phase, the hands manipulate and interact with the object according to the action defined through the textual prompt. We obtain the training data for this phase in a similar way as the grasping phase based on object pose heuristics. We employ a \mathbf{x}_0 diffusion model in a classifier-free manner (see Section 3), i.e., we directly predict the denoised output. This is shown to result in less noisy, higher quality motion than ϵ_θ (but less susceptibility to guidance) [Karunratanakul et al. 2023], which is critical during the interaction phase where the hand-object interaction takes place. Our training loss is given by

$$\mathbb{E}_{\epsilon \sim \mathcal{N}(0,1), t} \|\mathbf{x}_{0,\theta}(\mathbf{x}_t, \mathcal{T}, \mathcal{M}, t) - \mathbf{x}_0\|_2^2. \quad (6)$$

4.2.3 Grasp to Interaction Stage Transition. Maintaining a seamless transition between the grasping and interaction outputs is critical to generating realistic motion sequences. We rely on inference-time guidance [Karunratanakul et al. 2023] and motion imputing on the interaction model to achieve a smooth transition. To this end, the interaction diffusion model is trained to generate the complete sequence (including grasping). We then impute the entire sequence generated by the (guided) grasping model to the start of the interaction sequence and apply guidance. To perform the imputation we define respectively the projections P_g^x and P_{ss}^x that resize the grasp reference \mathbf{h}_g or sub-sequence poses \mathbf{h}_{ss} to that of \mathbf{x}_0 by filling in zeros. Similarly, M_g^x and M_{ss}^x represents the imputation regions of the grasp reference and sub-sequence on \mathbf{x}_0 . At each denoising step, the imputed denoised output, $\tilde{\mathbf{x}}_{0,\theta}$, is given by

$$\tilde{\mathbf{x}}_{0,\theta} = (1 - M_\tau^x) \odot \mathbf{x}_{0,\theta} + M_\tau^x \odot P_\tau^x \mathbf{h}_\tau, \quad (7)$$

where $\tau \in [g, ss]$ and \odot represents elementwise multiplication. We use the classifier guidance mechanism described in Sec. 3.1 and approximate the gradient signal for sub-sequence guidance as

$$\nabla_{\mathbf{x}_t} \log p(\mathbf{c}|\mathbf{x}_t) \approx -\nabla_{\mathbf{h}_t} \|\mathbf{h}_{ss} - \tilde{\mathbf{h}}_{ss}\|_2^2, \quad (8)$$

where \mathbf{h}_{ss} denotes the set of grasping poses and $\tilde{\mathbf{h}}_{ss}$ denotes the generated grasping poses from the grasping diffusion model. We show in Sec. 5.6 that this technique leads to a smoother transition between pre- and interaction compared to a single frame transition.

4.3 Grasp Guidance

To add controllability to the generation and improve generalization to unseen objects, we introduce grasp guidance for the grasping phase, which can be optionally be added at inference time. We leverage a single grasp frame, defined as the last frame of the grasping phase, that provides a prior about how and with which hand an object should roughly be grasped. Such a grasp can be obtained from motion capture or from an off-the-shelf hand-object pose estimator [Pavlakos et al. 2023] as demonstrated in Sec. 5.8. We provide inference-time guidance $G(\mathcal{H}_l, \mathcal{H}_r) = 0$ to our trained diffusion model to grasp the object in a pre-defined manner. More specifically, we approximate the gradient of the guidance signal in Eq. 4 as

$$\nabla_{\mathbf{x}_t} \log p(\mathbf{c}|\mathbf{x}_t) \approx -\nabla_{\mathbf{h}} \|\mathbf{h}_g - \hat{\mathbf{h}}_g\|_2^2, \quad (9)$$

where $\mathbf{h}_g \in (\mathcal{H}_l, \mathcal{H}_r)$ is the hand(s) pose in the last frame of the grasping sequence, and $\hat{\mathbf{h}}_g$ is the pre-defined grasp pose.

	Method	Backbone	SD [m] (↑)	OD [m](↑)	IV [cm^3] (↓)	ID [mm] (↓)	CR (↑)	MM (→)	DIV (→)	Hand Act. Rec. Acc. (↑)	Hand+Object Act. Rec. Acc. (↑)
Unseen subject split	Real Mocap (GRAB)	-	-	0.183	5.65	5.89	0.08	0.22	1.06	0.708	0.729
	IMoS [Ghosh et al. 2023]	CVAE	0.002	0.149	7.14	11.47	0.05	0.25	1.02	0.579	0.588
	DiffH ₂ O	Transformer	0.088	0.185	6.65	8.39	0.067	0.33	1.09	0.760	0.810
	DiffH ₂ O	UNet	0.109	0.188	6.02	7.92	0.064	0.30	1.08	0.833	0.875
Unseen object split	Real Mocap (GRAB)	-	-	0.183	3.40	5.63	0.071	0.20	1.08	0.683	0.784
	IMoS* [Ghosh et al. 2023]	CVAE	0.002	0.132	10.38	12.45	0.048	0.22	1.05	0.561	0.581
	DiffH ₂ O	Transformer	0.133	0.185	7.99	10.87	0.073	0.24	1.09	0.750	0.803
	DiffH ₂ O	UNet	0.134	0.179	9.03	11.39	0.086	0.23	1.09	0.755	0.837

Table 1. **Comparison to the State-of-the-Art in Postgrasp.** We compare our method with two backbone variants (MDM’s transformer and GMD’s UNet) against IMoS [Ghosh et al. 2023]. We also include real motion capture sequences from GRAB [Taheri et al. 2020] as reference. We present action recognition results using only hands as input, and using hands and objects in combination. We report results on an unseen subject split (top 4 rows), following [Ghosh et al. 2023], and on our unseen object test dataset (bottom 4 rows). For IMoS, we use the same pretrained model, which is trained on unseen subject split, across all our experiments (unseen subject/object splits). This is due to difficulties in reproducing training performance for the unseen object split, and is indicated with a * in the table (IMoS*). ↑ denotes higher values are better, ↓ denotes lower values are better, and → denotes values closer to ground-truth are better.

4.4 Textual Augmentations

Our model generates hand-object interactions based on textual inputs. To the best of our knowledge, there is currently no hand-object interaction dataset that contains detailed textual descriptions. For instance, the GRAB dataset [Taheri et al. 2020] only provides categorical action labels. To address this limitation, we auto-generated sentences using the template “the person <verb> + <object>” [Ghosh et al. 2023] (referred to as “simple” text). However, these sentences lack detailed information, which limits the controllability of the model via textual inputs. Therefore, we contribute carefully annotated textual descriptions of the GRAB dataset (referred to as “detailed” sentences). We instructed our annotators to carefully watch each ground truth video and describe the actions in three distinct stages of *pre-action*, *action*, and *post-action*. These descriptions are further augmented with hand and positional information. An example from the dataset is as follows: “The person picks up the apple with the right hand, passes it to their left hand, and then places it back with their right hand”. These detailed descriptions enhance the dataset, enabling more accurate evaluation and precise control of hand-object interactions as we show in Sec. 5.7.

5 EXPERIMENTS AND RESULTS

5.1 Baselines

Our method focuses on synthesizing detailed hand-object motion based on text input. To the best of our knowledge, DiffH₂O is the first method to tackle this problem. While there is no direct baseline for hand-object motion synthesis based on language, the closest to our approach is IMoS [Ghosh et al. 2023], which focuses on text-based whole-body human-object interaction synthesis. IMoS first generates a body articulation based on an instruction label (action + object), and then optimizes for the object pose using a grasp heuristic. Since our paper focuses on hand articulations and object motions, we omit the full-body movements from our evaluations.

To compare our method against human-body diffusion models, we adopted these methods to the HOI setting. All variants use our proposed representation. MDM [Tevet et al. 2023] does not use guidance, and for GMD [Karunratanakul et al. 2023] we use gradients to guide the model towards the grasp frame, but omit the 2D-trajectory generation stage because it is specific to human motions.

5.2 Data

GRAB: We utilize the subject-based split of the GRAB dataset [Taheri et al. 2020] proposed in IMoS to run a direct comparison. However, as this split does not contain unseen objects, we also create a new split featuring unseen objects based on the criteria of object similarity and semantics (see supplemental material for details).

HO-3D: To further evaluate guidance and object generalization, we estimate hand-object poses on the HO-3D dataset [Hampali et al. 2020] and guide our model to an estimated target pose.

5.3 Evaluation Metrics

Following previous works on motion synthesis [Braun et al. 2024; Ghosh et al. 2023; Taheri et al. 2022; Tendulkar et al. 2023], we report several physics-based metrics and evaluate our model’s accuracy through metrics that assess motion diversity and action features.

Physics Based Metrics: We report the interpenetration volume (IV) as the amount of MANO vertices that penetrate the object mesh and the maximum interpenetration depth (ID). Furthermore, we compute the contact ratio (CR) as the average ratio of hand vertices that are in contact, which is defined as points within a 5mm threshold of the object mesh.

Motion Diversity Metrics: We report the sample diversity (SD) between wrist trajectories in motion space. We sample the same input conditions five times and compute the pairwise Euclidean distance between the samples. We then report the mean sample diversity over all test prompts. We also provide the overall diversity (OD), which measures the pairwise Euclidean distance between all test samples. Since the wrist positions are normalized with respect to the initial object pose, no further normalization is applied.

Guidance Metrics: To assess how well the models adhere to the guidance signal, we report the mean error between the predictions and the reference grasp (GE), the ratio at which the diffusion model maintains the correct handedness according to the reference (HA). Furthermore, we evaluate the wrist velocities at the transition between grasping and interaction phase (T_{vel}).

Action Feature Based Metrics: To assess the naturalness and variety of the generated motions, we use the action recognition accuracy, diversity, and multimodality metrics, following [Ghosh et al. 2023]. We provide additional metrics (e.g. FID, KID), standard deviations and details about how these metrics are computed in our supplemental material.

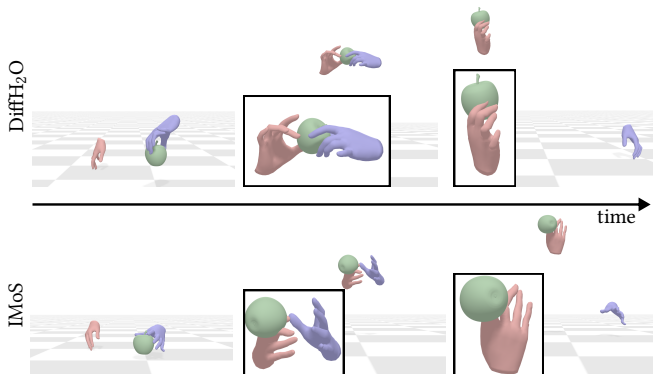


Fig. 3. **Qualitative Comparison.** Post-optimizing object motion as shown in IMoS [Ghosh et al. 2023] (bottom row) can exhibit artifacts with fine-grained manipulations, e.g., when an object switches hands. In contrast, our approach (top row) can seamlessly handle such scenarios. Best seen in the supplemental video.

5.4 Comparison to the State-of-the-Art

We conduct a set of experiments to compare to relevant baselines quantitatively. To demonstrate the generality of our method, we present qualitative examples of our method in Fig. 3 and supplementary materials (along with failure cases).

Setting 1 - Interaction Only: We compare our approach against the state-of-the-art human-object motion synthesis approach of IMoS in their postgrasp-only setting and report results in Tab. 1. To ensure a fair comparison in this experiment, no grasping and neither grasp guidance nor our detailed text annotations are used. We test our hand-object representation with two backbones, MDM’s transformer [Tevet et al. 2023] and GMD’s UNet [Karunratanakul et al. 2023]. Our model significantly outperforms IMoS across all physics and motion diversity metrics as well as on the action recognition accuracies. In particular, our method yields motions that are significantly more diverse (higher SD and OD), exhibit less interpenetration (lower IV and ID), and encode motion features that align with action type (higher action recognition accuracies). Note that IMoS assumes the availability of a ground-truth test motion to initialize the first few frames with it, while ours predicts the entire sequence. Yet, our approach achieves considerable performance improvements. While IMoS provides compelling realistic full body synthesis results, fine-grained finger motions as well as post-optimized object motions lag behind the realism and diversity demonstrated by our method, as shown in Fig. 3 and in our supplementary video. The higher scores of DiffH₂O compared to real mocap from the GRAB dataset in Tab. 1 can occur because the action classifier is trained on GRAB’s training-split, which is the distribution our model covers, whereas some of the test sequences in GRAB (real mocap) have quite distinct motions that the classifier may misclassify. However, the high scores demonstrate the representative power of DiffH₂O for generating realistic hand-object sequences that capture inherent motion and action semantics. Our method with a UNet backbone outperforms a transformer backbone in most metrics, which is in line with GMD’s findings that UNet

Method	IV [cm^3] (\downarrow)	GE [m] (\downarrow)	HA (\uparrow)	T _{vel} [$\frac{m}{s}$] (\downarrow)
MDM	8.98	0.38	0.45	0.14
GMD	9.03	0.49	0.46	12.68
Ours	7.40	0.12	0.87	0.23

Table 2. **Comparison to Diffusion Baselines for the Full Sequence.**

works better in low-data regimes. To assess the action recognition accuracy, we train two models, one that uses only hand 3D joints as input and another incorporating object 3D position as additional input. We demonstrate that DiffH₂O’s synthesized object motions contribute to larger performance improvements compared to the post-optimized motions computed by IMoS (8.2% improvement for ours vs 2% for IMoS) as shown in Tab. 1. This confirms the benefits of jointly modeling hand-object motion instead of decoupling it into separate components.

Setting 2 - Grasping + Interaction: In this experiment, we switch to the setting of generating the whole sequence of grasping and interaction, and are interested how well the models can be guided while generating high quality motions (without physical artifacts). We report results in Tab. 2 and find that our method outperforms baselines from human motion diffusion. In particular, our method better adheres to the grasp frame in terms of grasp error (GE) and handedness accuracy (HA), and achieves more natural grasps (lower IV). This justifies our contributions of two-stage separation and subsequence guidance over previous diffusion models.

5.5 Perceptual Study

To evaluate the visual quality of our motions, we conducted a perceptual user study on a set of 21 participants, who were randomly assigned one of four sets, each consisting of 30 randomly selected sequences. We compared our approach against IMoS. We displayed results from our method and IMoS side-by-side in random order, along with the input sentence description used to synthesize motions. We asked the following questions to the participants: “Which sequence is more realistic?” and “Which sequence has more variety in motion?”. We defined a sequence to be more realistic if the overall motion looks human-like, e.g., if the objects are grasped realistically and there are less artifacts such as floating objects or interpenetration. Moreover, a sequence has more variety if the object is manipulated multiple times and in distinct ways. In 63.1% of the responses, participants selected our method as the most realistic compared to IMoS. Even more distinctively, in 72.9% of the responses, participants favored our method to contain more variety than IMoS. We obtained statistically significant Fleiss’ kappa scores [Fleiss 1971] of 0.34 and 0.43 for Realism and Diversity, respectively, at $p < 0.05$. Please see supplemental material for more details.

5.6 Ablation Studies

We perform several ablations to justify our technical contributions. To evaluate the controllability gained through guidance, we compare our final method with several variants in Tab. 3. We use a base model which indicates a single stage model without guidance. We then gradually add our contributions, first the grasping and interaction task separation (2-ST), the grasp guidance (GG) and the sub-sequence guidance in the interaction phase (SS) as described in

Component			Metrics			
2-ST	KF	SS	IV [cm^3] (\downarrow)	KE [m] (\downarrow)	HA \uparrow	T_{vel} [$\frac{m}{s}$] (\downarrow)
×	×	×	7.48	0.31	0.52	0.21
✓	×	×	9.03	0.49	0.46	12.68
✓	✓	×	8.52	0.06	0.97	5.37
✓	✓	✓	7.40	0.12	0.87	0.23

Table 3. **Ablation Study.** We provide ablations of our components against the base model MDM [Tevet et al. 2023]. We measure the keyframe error (KE) and the accuracy of handedness (HA) with respect to the keyframe reference grasp, as well as interpenetration volume (IV). We also provide the wrist joint velocities (T_{vel}) for the transition from grasping to interaction.

Pose Representation	Metrics		
	IV [cm^3] (\downarrow)	ID [mm] (\downarrow)	CR \uparrow
D-Grasp [Christen et al. 2022]	5.56	8.60	0.055
Ours w/o SDF	10.79	11.42	0.073
Ours w/ object-relative pose	9.38	11.41	0.077
Ours w/ first frame relative pose (Ours)	9.03	11.39	0.086

Table 4. **Pose Representation Evaluation.** We compare different alternative pose representations and demonstrate the benefits of object-relative pose representation and encoding hand-object signed distances.

Sec. 4.2. As expected, the grasp reference is being ignored without guidance (top 2 rows in Tab. 3), leading to high grasp errors and low hand correctness. Adding guidance allows for better performance in grasp error and hand accuracy, however, a high T_{vel} indicates a sudden jump of the hands between grasping and interaction. To mitigate this, we introduce the smooth transition technique that leads to the best overall score at the cost of a slight increase in grasp error and decrease in hand correctness. The interpenetration volume is lowest with our final model, indicating the best generalization to unseen objects. To validate our canonicalized representation, we compare against a variant inspired by D-Grasp [Christen et al. 2022], our representation without SDF, using object-relative positions at every step, and finally our representation of object-relative with regards to the initial frame. Our final representation achieves less interpenetration and better contact modeling.

5.7 Controllability via Text Prompts

In this experiment, we train DiffH₂O once with our detailed text labels and once with simple text prompts generated from the GRAB objects and action labels. As shown in Tab. 5, our textual descriptions offer significant advantage by enabling control over handedness. To gauge controllability, we measure whether the active hand in the generated motion corresponds to prompted hand. Our model, trained with detailed text annotations achieves a correct overall handedness accuracy of 86.5% against 59.3% accuracy when trained with simple text prompts. We see a performance drop when training on detailed texts and testing on simple texts (0.731) and vice-versa, which was similarly observed in [Shvetsova et al. 2023] due to a style gap. Similarly, we measure action correctness by evaluating the match ratio between the prompted action and the action demonstrated in the generated motion. Using detailed textual descriptions enables our model to generate motions that align more accurately with the text input, demonstrated by a 93.5% accuracy compared to the 54.8% accuracy achieved by our model tested with simple

Train Input	Test Input	Action Correctness	Hand correctness			Total	Cosine Similarity
			Right	Left	Both		
simple	simple	0.897	n/a	n/a	n/a	n/a	0.72
detailed	simple	0.731	n/a	n/a	n/a	n/a	0.43
simple	detailed	0.548	0.709	0.111	0.0	0.593	0.43
detailed	detailed	0.935	0.869	0.862	0.75	0.865	0.66

Table 5. **Text evaluation.** We demonstrate that comprehensive text descriptions enable us to generate motions more representative of the description, and allow fine-grained controllable hand-object motion synthesis.

text descriptions. Since the test inputs are much more diverse with the detailed textual descriptions, this furthermore demonstrates the robustness to unseen sentences. We also report the cosine similarity between the different sets of texts as a reference.

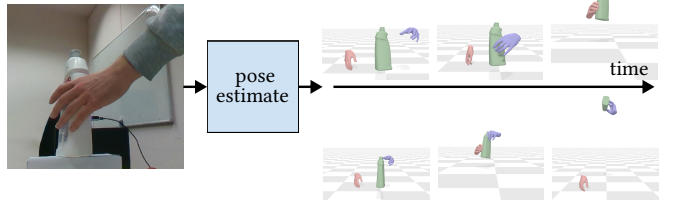


Fig. 4. **Generation from Pose Estimate.** We use an off-the-shelf image based pose estimator to provide a keyframe grasp. Our model then generates a variety of different actions that pass through the provided hand pose.

5.8 Motion Generation from Estimated Pose

We run an image-based pose estimator [Pavlakos et al. 2023] on single images from HO3D [Hampali et al. 2020] to obtain object-relative hand poses. We then use these hand poses as reference grasps and pass them through our diffusion framework together with multiple different textual descriptions. This highlights the practicality of our framework-given a single grasp reference, we can generate multiple diverse sequences.

6 DISCUSSION AND CONCLUSION

In this work, we have introduced a framework to generate plausible hand-object interactions from textual descriptions. Specifically, we have proposed a two-stage diffusion method that separates sequences into a grasping and interaction stage and uses single keyframe grasps as guidance to the diffusion model to improve generalization across unseen objects. Through our compact representation, hands are coupled to object motions resulting in realistic interactions. While we provide a first step towards object generalization, there are limitations of our framework. To remove physical artifacts, physics could be explicitly integrated into the diffusion process [Yuan et al. 2023]. The inference time is still relatively slow in diffusion models. To increase efficiency, operating in latent space is an interesting direction to explore [Chen et al. 2023a]. Lastly, grasp references for guidance which are far away from the training distribution tend to be ignored by our model. Therefore, exploring new ways to guide the diffusion model towards out-of-distribution samples is a crucial future research direction.

REFERENCES

- Anonymous. 2023. GeneOH Diffusion: Towards Generalizable Hand-Object Interaction Denoising via Denoising Diffusion. In *Submitted to The Twelfth International Conference on Learning Representations*. <https://openreview.net/forum?id=FvK2noilxT> under review.
- Nikos Athanasiou, Mathis Petrovich, Michael J Black, and Gül Varol. 2022. Teach: Temporal action composition for 3d humans. In *International Conference on 3D Vision (3DV)*. IEEE, 414–423.
- Samarth Brahmabhatt, Cusuh Ham, Charles C Kemp, and James Hays. 2019. Contactdb: Analyzing and predicting grasp contact via thermal imaging. In *Computer Vision and Pattern Recognition (CVPR)*. 8709–8719.
- Samarth Brahmabhatt, Chengcheng Tang, Christopher D Twigg, Charles C Kemp, and James Hays. 2020. ContactPose: A dataset of grasps with object contact and hand pose. In *European Conference on Computer Vision (ECCV)*. Springer, 361–378.
- Jona Braun, Sammy Christen, Muhammed Kocabas, Emre Aksan, and Otmar Hilliges. 2024. Physically Plausible Full-Body Hand-Object Interaction Synthesis. In *International Conference on 3D Vision (3DV)*.
- Yu-Wei Chao, Wei Yang, Yu Xiang, Pavlo Molchanov, Ankur Handa, Jonathan Tremblay, Yashraj S. Narang, Karl Van Wyk, Umar Iqbal, Stan Birchfield, Jan Kautz, and Dieter Fox. 2021. DexYCB: A Benchmark for Capturing Hand Grasping of Objects. In *Computer Vision and Pattern Recognition (CVPR)*.
- Sirui Chen, Albert Wu, and C. Karen Liu. 2023b. Synthesizing Dexterous Nonprehensile Pregrasp for Ungraspable Objects. In *ACM SIGGRAPH 2023 Conference Proceedings (Los Angeles, CA, USA) (SIGGRAPH '23)*. Association for Computing Machinery, New York, NY, USA, Article 10, 10 pages. <https://doi.org/10.1145/3588432.3591528>
- Xin Chen, Biao Jiang, Wen Liu, Zilong Huang, Bin Fu, Tao Chen, and Gang Yu. 2023a. Executing your Commands via Motion Diffusion in Latent Space. In *Proceedings of the IEEE/CVF Conference on Computer Vision and Pattern Recognition*. 18000–18010.
- Min Jin Chong and David Forsyth. 2020. Effectively unbiased fid and inception score and where to find them. In *Proceedings of the IEEE/CVF conference on computer vision and pattern recognition*. 6070–6079.
- Sammy Christen, Muhammed Kocabas, Emre Aksan, Jemin Hwangbo, Jie Song, and Otmar Hilliges. 2022. D-Grasp: Physically Plausible Dynamic Grasp Synthesis for Hand-Object Interactions. In *Computer Vision and Pattern Recognition (CVPR)*.
- Jia Deng, Wei Dong, Richard Socher, Li-Jia Li, Kai Li, and Li Fei-Fei. 2009. Imagenet: A large-scale hierarchical image database. In *Computer Vision and Pattern Recognition (CVPR)*. Ieee, 248–255.
- Prafulla Dhariwal and Alexander Nichol. 2021. Diffusion models beat gans on image synthesis. *Advances in neural information processing systems* 34 (2021), 8780–8794.
- Christian Diller and Angela Dai. 2023. CG-HOI: Contact-Guided 3D Human-Object Interaction Generation. *arXiv preprint arXiv:2311.16097* (2023).
- Zicong Fan, Omid Taheri, Dimitrios Tzionas, Muhammed Kocabas, Manuel Kaufmann, Michael J. Black, and Otmar Hilliges. 2023. ARCTIC: A Dataset for Dexterous Bimanual Hand-Object Manipulation. In *Computer Vision and Pattern Recognition (CVPR)*.
- Joseph L Fleiss. 1971. Measuring nominal scale agreement among many raters. *Psychological bulletin* (1971).
- Guillermo Garcia-Hernando, Edward Johns, and Tae-Kyun Kim. 2020. Physics-based dexterous manipulations with estimated hand poses and residual reinforcement learning. In *International Conference on Robotics and Automation (ICRA)*. IEEE, 9561–9568.
- Anindita Ghosh, Rishabh Dabral, Vladislav Golyanik, Christian Theobalt, and Philipp Slusallek. 2023. IMoS: Intent-Driven Full-Body Motion Synthesis for Human-Object Interactions. In *Eurographics*.
- Chuan Guo, Xinxin Zuo, Sen Wang, Shihao Zou, Qingyao Sun, Annan Deng, Mingjun Gong, and Li Cheng. 2020. Action2motion: Conditioned generation of 3d human motions. In *Proceedings of the 28th ACM International Conference on Multimedia*. 2021–2029.
- Shreyas Hampali, Mahdi Rad, Markus Oberweger, and Vincent Lepetit. 2020. HOnnotate: A method for 3D Annotation of Hand and Object Poses. In *Computer Vision and Pattern Recognition (CVPR)*.
- Mohamed Hassan, Yunrong Guo, Tingwu Wang, Michael Black, Sanja Fidler, and Xue Bin Peng. 2023. Synthesizing Physical Character-scene Interactions. In *International Conference on Computer Graphics and Interactive Techniques (SIGGRAPH)*.
- Jonathan Ho, Ajay Jain, and Pieter Abbeel. 2020. Denoising diffusion probabilistic models. *Advances in neural information processing systems* 33 (2020), 6840–6851.
- Jonathan Ho and Tim Salimans. 2022. Classifier-free diffusion guidance. *NeurIPS 2021 Workshop on Deep Generative Models and Downstream Applications*: (2022).
- Jonathan Ho, Tim Salimans, Alexey Gritsenko, William Chan, Mohammad Norouzi, and David J Fleet. 2022. Video diffusion models. *arXiv:2204.03458* (2022).
- Siyuan Huang, Zan Wang, Puhao Li, Baoxiong Jia, Tengyu Liu, Yixin Zhu, Wei Liang, and Song-Chun Zhu. 2023. Diffusion-based Generation, Optimization, and Planning in 3D Scenes. *arXiv:2301.06015* [cs.CV]
- Sadeep Jayasumana, Srikumar Ramalingam, Andreas Veit, Daniel Glasner, Ayan Chakrabarti, and Sanjiv Kumar. 2023. Rethinking FID: Towards a Better Evaluation Metric for Image Generation. *arXiv:2401.09603* [cs.CV]
- Korrawe Karunratanakul, Konpat Preechakul, Supasorn Suwajanakorn, and Siyu Tang. 2023. Guided Motion Diffusion for Controllable Human Motion Synthesis. In *Proceedings of the IEEE/CVF International Conference on Computer Vision*. 2151–2162.
- Manuel Kaufmann, Velko Vechev, and Dario Mylonopoulos. 2022. *aitviewer*. <https://doi.org/10.5281/zenodo.10013305>
- Zhifeng Kong, Wei Ping, Jiayi Huang, Kexin Zhao, and Bryan Catanzaro. 2021. DiffWave: A Versatile Diffusion Model for Audio Synthesis. In *International Conference on Learning Representations*. <https://openreview.net/forum?id=a-xFK8Ymz5J>
- Taein Kwon, Bugra Tekin, Jan Stühmer, Federica Bogo, and Marc Pollefeys. 2021. H2O: Two Hands Manipulating Objects for First Person Interaction Recognition. In *International Conference on Computer Vision (ICCV)*. 10138–10148.
- Jiye Lee and Hanbyul Joo. 2023. Locomotion-Action-Manipulation: Synthesizing Human-Scene Interactions in Complex 3D Environments. *arXiv:2301.02667* [cs.CV]
- Rosario Leonardi, Antonino Furnari, Francesco Ragusa, and Giovanni Maria Farinella. 2023. Are Synthetic Data Useful for Egocentric Hand-Object Interaction Detection? An Investigation and the HOI-Synth Domain Adaptation Benchmark. *arXiv preprint arXiv:2312.02672* (2023).
- Jiaman Li, Alexander Clegg, Roozbeh Mottaghi, Jiajun Wu, Xavier Puig, and C Karen Liu. 2023. Controllable Human-Object Interaction Synthesis. *arXiv preprint arXiv:2312.03913* (2023).
- Quanzhou Li, Jingbo Wang, Chen Change Loy, and Bo Dai. 2024. Task-oriented human-object interactions generation with implicit neural representations. In *Proceedings of the IEEE/CVF Winter Conference on Applications of Computer Vision*. 3035–3044.
- Yunze Liu, Yun Liu, Che Jiang, Kangbo Lyu, Weikang Wan, Hao Shen, Boqiang Liang, Zhoujie Fu, He Wang, and Li Yi. 2022. HOI4D: A 4D Egocentric Dataset for Category-Level Human-Object Interaction. In *Computer Vision and Pattern Recognition (CVPR)*. 21013–21022.
- Zhengyi Luo, Ryo Hachiuma, Ye Yuan, and Kris Kitani. 2021. Dynamics-regulated kinematic policy for egocentric pose estimation. *Advances in Neural Information Processing Systems* 34 (2021), 25019–25032.
- Naureen Mahmood, Nima Ghorbani, Nikolaus F. Troje, Gerard Pons-Moll, and Michael J. Black. 2019. AMASS: Archive of Motion Capture as Surface Shapes. In *International Conference on Computer Vision*. 5442–5451.
- Priyanka Mandikal and Kristen Grauman. 2021. Learning Dexterous Grasping with Object-Centric Visual Affordances. In *International Conference on Robotics and Automation (ICRA)*.
- Alexander Quinn Nichol and Prafulla Dhariwal. 2021. Improved denoising diffusion probabilistic models. In *International Conference on Machine Learning*. PMLR, 8162–8171.
- Atsuhiro Noguchi and Tatsuya Harada. 2019. Image generation from small datasets via batch statistics adaptation. In *Proceedings of the IEEE/CVF International Conference on Computer Vision*. 2750–2758.
- Georgios Pavlakos, Dandan Shan, Ilija Radosavovic, Angjoo Kanazawa, David Fouhey, and Jitendra Malik. 2023. Reconstructing Hands in 3D with Transformers. In *arxiv*.
- Xiaogang Peng, Yiming Xie, Zizhao Wu, Varun Jampani, Deqing Sun, and Huaizu Jiang. 2023. HOI-Diff: Text-Driven Synthesis of 3D Human-Object Interactions using Diffusion Models. *arXiv preprint arXiv:2312.06553* (2023).
- Sergey Prokudin, Christoph Lassner, and Javier Romero. 2019. Efficient learning on point clouds with basis point sets. In *Computer Vision and Pattern Recognition (CVPR)*. 4332–4341.
- Yuzhe Qin, Yueh-Hua Wu, Shaowei Liu, Hanwen Jiang, Ruihan Yang, Yang Fu, and Xiaolong Wang. 2021. DexMV: Imitation Learning for Dexterous Manipulation from Human Videos. *arXiv preprint arXiv:2108.05877* (2021).
- Alec Radford, Jong Wook Kim, Chris Hallacy, Aditya Ramesh, Gabriel Goh, Sandhini Agarwal, Girish Sastry, Amanda Askell, Pamela Mishkin, Jack Clark, et al. 2021. Learning transferable visual models from natural language supervision. In *International conference on machine learning*. PMLR, 8748–8763.
- Aravind Rajeswaran, Vikash Kumar, Abhishek Gupta, Giulia Vezzani, John Schulman, Emanuel Todorov, and Sergey Levine. 2018. Learning Complex Dexterous Manipulation with Deep Reinforcement Learning and Demonstrations. In *Robotics: Science and Systems (RSS)*.
- Robin Rombach, Andreas Blattmann, Dominik Lorenz, Patrick Esser, and Björn Ommer. 2022. High-resolution image synthesis with latent diffusion models. In *Proceedings of the IEEE/CVF conference on computer vision and pattern recognition*. 10684–10695.
- Javier Romero, Dimitrios Tzionas, and Michael J. Black. 2017. Embodied Hands: Modeling and Capturing Hands and Bodies Together. *Transactions on Graphics (TOG)* 36, 6 (Nov. 2017).
- Qijin She, Ruizhen Hu, Juzhan Xu, Min Liu, Kai Xu, and Hui Huang. 2022. Learning High-DOF Reaching-and-Grasping via Dynamic Representation of Gripper-Object Interaction. *Transactions on Graphics (TOG)* 41, 4 (2022), 97:1–97:14.
- Soshi Shimada, Franziska Mueller, Jan Bednarik, Bardia Doosti, Bernd Bickel, Danhang Tang, Vladislav Golyanik, Jonathan Taylor, Christian Theobalt, and Thabo Beeler. 2023. Macs: Macs conditioned 3d hand and object motion synthesis. *arXiv preprint arXiv:2312.14929* (2023).

- Nina Shvetsova, Anna Kukleva, Bernt Schiele, and Hilde Kuehne. 2023. In-Style: Bridging Text and Uncurated Videos with Style Transfer for Text-Video Retrieval. *International Conference on Computer Vision (ICCV)* (2023).
- Jascha Sohl-Dickstein, Eric Weiss, Niru Maheswaranathan, and Surya Ganguli. 2015. Deep unsupervised learning using nonequilibrium thermodynamics. In *International conference on machine learning*. PMLR, 2256–2265.
- Omid Taheri, Vasileios Choutas, Michael J. Black, and Dimitrios Tzionas. 2022. GOAL: Generating 4D Whole-Body Motion for Hand-Object Grasping. In *Computer Vision and Pattern Recognition (CVPR)*. <https://goal.is.tue.mpg.de>
- Omid Taheri, Nima Ghorbani, Michael J. Black, and Dimitrios Tzionas. 2020. GRAB: A Dataset of Whole-Body Human Grasping of Objects. In *European Conference on Computer Vision (ECCV)*. <https://grab.is.tue.mpg.de>
- Purva Tendulkar, Didac Suris, and Carl Vondrick. 2023. FLEX: Full-Body Grasping Without Full-Body Grasps. In *Computer Vision and Pattern Recognition (CVPR)*.
- Guy Tevet, Sigal Raab, Brian Gordon, Yoni Shafir, Daniel Cohen-or, and Amit Haim Bermano. 2023. Human Motion Diffusion Model. In *The Eleventh International Conference on Learning Representations*. <https://openreview.net/forum?id=SJ1kSyO2jwu>
- Jingbo Wang, Sijie Yan, Bo Dai, and Dahua Lin. 2021. Scene-aware generative network for human motion synthesis. In *Computer Vision and Pattern Recognition (CVPR)*. 12206–12215.
- Yan Wu, Jiahao Wang, Yan Zhang, Siwei Zhang, Otmar Hilliges, Fisher Yu, and Siyu Tang. 2022. SAGA: Stochastic Whole-Body Grasping with Contact. In *Proceedings of the European Conference on Computer Vision (ECCV)*.
- Sirui Xu, Zhengyuan Li, Yu-Xiong Wang, and Liang-Yan Gui. 2023. InterDiff: Generating 3D Human-Object Interactions with Physics-Informed Diffusion. In *International Conference on Computer Vision (ICCV)*.
- Ling Yang, Zhilong Zhang, Yang Song, Shenda Hong, Runsheng Xu, Yue Zhao, Wentao Zhang, Bin Cui, and Ming-Hsuan Yang. 2023. Diffusion models: A comprehensive survey of methods and applications. *Comput. Surveys* 56, 4 (2023), 1–39.
- Yufei Ye, Poorvi Hebbar, Abhinav Gupta, and Shubham Tulsiani. 2023a. Diffusion-Guided Reconstruction of Everyday Hand-Object Interaction Clips. In *International Conference on Computer Vision (ICCV)*.
- Yufei Ye, Xueting Li, Abhinav Gupta, Shalini De Mello, Stan Birchfield, Jiaming Song, Shubham Tulsiani, and Sifei Liu. 2023b. Affordance Diffusion: Synthesizing Hand-Object Interactions. In *Computer Vision and Pattern Recognition (CVPR)*.
- Yuting Ye and C Karen Liu. 2012. Synthesis of detailed hand manipulations using contact sampling. *Transactions on Graphics (TOG)* 31, 4 (2012), 1–10.
- Ye Yuan, Jiaming Song, Umar Iqbal, Arash Vahdat, and Jan Kautz. 2023. PhysDiff: Physics-Guided Human Motion Diffusion Model. In *International Conference on Computer Vision (ICCV)*.
- Hui Zhang, Sammy Christen, Zicong Fan, Luocheng Zheng, Jemin Hwangbo, Jie Song, and Otmar Hilliges. 2024. ArtiGrasp: Physically Plausible Synthesis of Bi-Manual Dexterous Grasping and Articulation. In *International Conference on 3D Vision (3DV)*.
- He Zhang, Yuting Ye, Takaaki Shiratori, and Taku Komura. 2021. Manipnet: neural manipulation synthesis with a hand-object spatial representation. *Transactions on Graphics (TOG)* 40, 4 (2021), 1–14.
- Lvmin Zhang, Anyi Rao, and Maneesh Agrawala. 2023. Adding conditional control to text-to-image diffusion models. In *Proceedings of the IEEE/CVF International Conference on Computer Vision*. 3836–3847.
- Mingyuan Zhang, Zhongang Cai, Liang Pan, Fangzhou Hong, Xinying Guo, Lei Yang, and Ziwei Liu. 2022b. MotionDiffuse: Text-Driven Human Motion Generation with Diffusion Model. *arXiv preprint arXiv:2208.15001* (2022).
- Xiaohan Zhang, Bharat Lal Bhatnagar, Sebastian Starke, Vladimir Guzov, and Gerard Pons-Moll. 2022a. COUCH: Towards Controllable Human-Chair Interactions. (October 2022).
- Juntian Zheng, Qingyuan Zheng, Lixing Fang, Yun Liu, and Li Yi. 2023. CAMS: CAnon-icalized Manipulation Spaces for Category-Level Functional Hand-Object Manipulation Synthesis. In *Proceedings of the IEEE/CVF Conference on Computer Vision and Pattern Recognition*. 585–594.
- Keyang Zhou, Bharat Lal Bhatnagar, Jan Eric Lenssen, and Gerard Pons-Moll. 2022. Toch: Spatio-temporal object-to-hand correspondence for motion refinement. In *European Conference on Computer Vision*. Springer, 1–19.
- Yi Zhou, Connelly Barnes, Jingwan Lu, Jimei Yang, and Hao Li. 2019. On the continuity of rotation representations in neural networks. In *Proceedings of the IEEE/CVF Conference on Computer Vision and Pattern Recognition*. 5745–5753.

Appendix - Supplementary Material

A IMPLEMENTATION DETAILS

DiffH₂O architecture is based on UNet with Adaptive Group Normalization (AdaGN) which was originally proposed in [Dhariwal and Nichol 2021] and also adapted in [Karunratanakul et al. 2023] for sequence prediction tasks. We adapt this network architecture for our two-stage design, that involves pre-grasp and post-grasp diffusion models. We provide the hyperparameter settings used in our architecture in Table 6.

B EXPERIMENTAL DETAILS

B.1 Training the action classifier.

We train a standard RNN action recognition classifier on the GRAB dataset and use the final layer of the classifier as the motion feature extractor for calculating action recognition accuracies as well as diversity (DIV) and multimodality (MM) scores, following [Ghosh et al. 2023] and [Guo et al. 2020]. We employ the online available code from IMoS and use the same network architecture and parameters to train our model.

B.2 Unseen object split

To assess our model’s ability to generalize to unseen classes, we also introduce a new split comprising unseen objects that were not present during training. Our test set is composed of the following objects: “apple, mug, train, elephant, alarm clock, small pyramid, medium cylinder and large torus”. Note that the training set includes pyramids, cylinders, and torus in other sizes. We exclude small pyramids, medium cylinders, and large torus from the training set to test our models’ ability to generalize to different sizes of the same objects

B.3 Details of the Action Recognition Evaluation Metrics.

Recognition Accuracy. Given a pretrained classifier, we input motions generated by DiffH₂O as well as our baselines and report top-1 percentage accuracy. The recognition accuracy indicates the correlation of the action type and the motion.

Diversity. We compute the diversity score by computing the variance of the features extracted from the action classifier across all action categories. Given a set of features extracted from generated motions across all action categories, two subsets with the same size, N , are randomly sampled. These features are denoted as $\{v_1, v_2, \dots, v_N\}$ for the first subset and $\{v'_1, v'_2, \dots, v'_N\}$ for the second subset. With $N = 200$, the diversity is defined as

$$DIV = \frac{1}{N} \sum_{i=1}^N \|v_i - v'_i\| \quad (10)$$

Multimodality. Different from the diversity metric, multimodality computes variance only within a specific action. An overall score is attained based on averaging the variances across all action types.

Fréchet Inception Distance (FID). FID is computed based on the (Fréchet) distance of the features of real ground-truth motions and generated motions. It has the assumption that the features computed

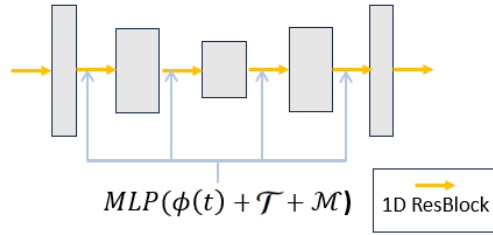


Fig. 5. **Overview of the diffusion architecture.** Our pipeline relies on a UNet block and processes three input signals: the time step $\phi(t)$, a text-prompt embedding \mathcal{T} and an object shape encoding \mathcal{M} . The time step is encoded using sinusoidal functions, the text-prompt embedding is generated by the CLIP text encoder model and the object encoding is obtained from BPS[Prokudin et al. 2019]. Similarly to [Karunratanakul et al. 2023], we use Adaptive Group normalization in 1D block

Parameter	Pre-Grasp Model	Post-grasp Model
Batch size	32	32
Base channels	256	512
Latent dimension	256	512
Channel multipliers	(1, 1, 1)	(2, 2, 2, 2)
β scheduler	Cosine [Nichol and Dhariwal 2021]	
Learning rate	1e-4	1e-4
Optimizer	AdamW (wd = 1e-2)	
Training T	400	
Diffusion loss	ϵ prediction	x_0 prediction
Diffusion var.	Fixed small $\hat{\beta}_t = \frac{1-\alpha_t-1}{1-\alpha_t} \beta_t$	
Model avg. beta	0.9999	

Table 6. **Network architecture.** Model and training hyperparameters of DiffH₂O

from the real data and synthesized data have a Gaussian distribution. Earlier work demonstrated that for small sample sizes, FID metric is biased and not stable.

Kernel Inception Distance (KID). KID metric relaxes the Gaussianity assumption and aims to improve upon FID. It measures the squared Maximum Mean Discrepancy (MMD) between the feature representations of the real and generated samples using a polynomial kernel. This metric has been found to be more robust when the sample size is small [Noguchi and Harada 2019].

B.4 Visualization Pipeline.

We use AITViewer [Kaufmann et al. 2022] to visualize motions synthesized by DiffH₂O as well as our baselines. IMoS synthesizes 15 frames of human-object interactions. They determine the hand which is in contact with the object according to GT, which can lead to a jump of the object from one hand to the other for certain actions. To make the frame rates comparable with DiffH₂O, we upsample the synthesis results of IMoS to 75 frames using spherical interpolation. Therefore, this jump may result in an artifact in which the object is floating from one hand to another.

C ADDITIONAL EXPERIMENTS

C.1 Action Recognition Experiments

Training action classifier on the whole GRAB data. IMoS [Ghosh et al. 2023] reports results using the whole dataset to train the action classifier on ground-truth motions and testing on the synthesized actions. Since their model initializes the sequences with ground-truth from the test data, this could positively bias their scores. Therefore, we omit test data from training, in our analysis in Table 1 of the main paper, both for our approach and IMoS. We show however in this supplemental material (Table 7) that our model is still able to outperform IMoS even when all the GRAB data, including test data, is included in training the classifier. This is a setup which is more favorable for IMoS as the first frame of synthesized IMoS motion comes from test data. This re-confirms the ability of our method to encode diverse motion features that represents realistic hand-object interactions.

FID and KID metrics. It’s been shown by earlier studies [Noguchi and Harada 2019], [Jayasumana et al. 2023], [Chong and Forsyth 2020] that Fréchet Inception Distance (FID) metric is biased and not stable for calculating the distances for small datasets. Since the GRAB subject split only contains 144 motions, in addition to FID, we also report the more stable Kernel Inception Distance (KID) metric which provides more reliable scores with fewer samples (Table 8). Table 8 also includes the standard deviations for the multimodality and diversity metrics based upon 20 repetitions of the evaluation.

Full-sequence training. Given an initial pose of the grasp moment, IMoS only synthesizes post-grasp sequences. To compare our results to IMoS in Table 1 of the main paper, we evaluated our models only on the post-grasp sequence part of the synthesis. In Table 9, we also provide diversity, multimodality, FID, KID and action recognition scores computed over the full sequence including pre- and post-grasp stages. We compare our results against real motions from ground-truth and demonstrate that we can achieve scores similar to ground-truth, which demonstrates our capability to synthesize realistic hand-object interactions.

C.2 Text Input Evaluation Experiments

In Table 10, we provide further details for the text input to the diffusion model. We first compare IMoS and our model trained on the subject split and tested on the object split. Notably, our model outperforms IMoS by 9.2% in action correctness, a significant improvement. When trained and tested on our unseen object splits, we find that our model remains competitive with IMoS. However, we notice that our model struggles with classes like apple and train, where new motions are introduced that differ from those in the training set. Our model must learn to generalize from eating bananas to apples, and while it achieves this, its performance decreases to 81.8%. Similarly, for the train class, our model’s accuracy drops to 50% since the unique motions of playing with a train were not observed during training. Nevertheless, our model demonstrates the ability to generalize to different object sizes, as it generates motions corresponding to recognizable actions for varied sizes of cylinders, pyramids, and torus in the training set.

Finally, we train and test our model with the augmented sentences we proposed for GRAB, leading to improved generalization, especially for the classes “train” and “apple”. These new sentences provide detailed motion descriptions, such as “The person picks up the train using their right hand, then rides it through the air close to the table surface, and finally puts it on the table using their right hand.” The augmented sentences enhance generalization and provide control over specifics like handedness, motion type, and physical location. Testing a model trained solely with baseline sentences on augmented sentences reveals a decrease in generalization, as anticipated. We observed a significant 38.7% performance gap between baseline and augmented sentences, showing the importance of text style. This highlights the limitations of relying solely on simple sentences for training and underscores the value of incorporating diverse and detailed descriptions to enhance model performance and generalization capabilities.

C.3 Detailed Investigation User Study

In our user study, we provide each user with 30 side-by-side comparisons. In our investigation, our model showed low realism but high diversity for the “pass” action, influenced by users perceiving “pass” action label in the GRAB dataset as transferring an object between hands, not to another person. In the “offhand” category, our model excelled in realism, while IMoS exhibited artifacts. This is due to the fact that IMoS determines the hand which is in contact with the object according to ground-truth, which leads to a jump of the object for the “off-hand” category.

C.4 More Qualitative Results and Failure Cases

We provide more qualitative results of our model with simple instructions in Fig. 6a, for grasp guidance in Fig. 6b, and with detailed instructions in Fig. 6c. Furthermore, we present three failure cases: the generated action does not match the text prompt (Fig. 7a), the grasp reference is ignored during guidance (Fig. 7b), or the hand in the text prompt is ignored (Fig. 7c).

D COMPUTATIONAL RESOURCES

The training of our model takes approximately 48 GPU hours on a single NVIDIA V100. Our model has a throughput of 32 samples per second. The total inference time for 32 samples is approximately 300 seconds.

	Method	Hand Act.	Hand+Object Act.	DIV (\rightarrow)	MM (\rightarrow)	KID (\downarrow)	FID (\downarrow)
		Rec. Accuracy (\uparrow)	Rec. Accuracy (\uparrow)				
Unseen subject split	Real Mocap	1.0	1.0	1.1358 \pm 0.0164	0.3105 \pm 0.0163	-	-
	IMoS [Ghosh et al. 2023]	0.7017	0.6754	1.1053 \pm 0.0128	0.2882 \pm 0.0114	0.005811	0.6267
	DiffH ₂ O	0.8125	0.9028	1.1440\pm0.0115	0.3176\pm0.0127	0.005346	0.8342
Unseen object split	Real Mocap	1.0	1.0	1.1324 \pm 0.0119	0.2355 \pm 0.0044	-	-
	IMoS* [Ghosh et al. 2023]	0.7161	0.8000	1.1173 \pm 0.0112	0.2513\pm0.0104	0.006038	0.7101
	DiffH ₂ O	0.7836	0.8125	1.1225\pm0.0120	0.2174 \pm 0.0074	0.005494	0.8821

Table 7. **Action feature based metrics using all training data [Ghosh et al. 2023].** We report action feature based metrics using action recognition models trained on pose data of all GRAB training data following the protocol of [Ghosh et al. 2023]. We either use a subject-based split (top 3 rows) or an object-based split (bottom 3 rows). \downarrow denotes lower values are better, and \rightarrow denotes values closer to the ground-truth are better. Our results achieves state-of-the-art accuracy across different metrics.

	Method	DIV (\rightarrow)	MM (\rightarrow)	KID (\downarrow)	FID (\downarrow)
	IMoS [Ghosh et al. 2023]	1.0237 \pm 0.0158	0.2538\pm0.0103	0.008065	0.6267
	DiffH ₂ O	1.0757\pm0.0129	0.3037 \pm 0.0079	0.006697	0.8342
Unseen object split	Ground-truth	1.0757 \pm 0.0129	0.2002 \pm 0.0063	-	-
	IMoS* [Ghosh et al. 2023]	1.0471 \pm 0.0129	0.2202\pm0.0093	0.008641	0.6593
	DiffH ₂ O	1.0942\pm0.0125	0.2307 \pm 0.0060	0.007503	0.8425

Table 8. **Details of the quantitative analysis with action feature based metrics.** We provide further details for the quantitative analysis in Table 1 of the main paper and report standard deviations of multimodality and diversity metrics as well as FID and KID scores. The results here are obtained using action recognition models trained on hand pose data of the respective training splits as indicated in the first column. We either use a subject-based split (top 3 rows) or an object-based split (bottom 3 rows). For IMoS, we use the same pretrained model, which is trained on unseen subject split, across all our experiments (unseen subject and unseen object splits) due to difficulties in reproducing training performance for the unseen object split (indicated with a * in the table, IMoS*). Therefore IMoS* sees a part of the unseen object test split during training the model which positively biases their score. \downarrow denotes lower values are better, and \rightarrow denotes values closer to the ground-truth are better. Our results achieves state-of-the-art accuracy across different metrics.

Method	Hand Act.	Hand+Object Act.	DIV (\rightarrow)	MM (\rightarrow)	KID (\downarrow)	FID (\downarrow)
	Rec. Accuracy (\uparrow)	Rec. Accuracy (\uparrow)				
Real Mocap (Full-sequence)	1.0	1.0	1.0983 \pm 0.0059	0.2235 \pm 0.0042	-	-
DiffH ₂ O (Full-sequence)	0.7720	0.8031	1.0948 \pm 0.0120	0.1555 \pm 0.0057	0.0067	0.7993

Table 9. **Action feature based metrics on full sequence synthesis.** We report action feature based metrics on our unseen object split using action recognition models trained on full sequences instead of only post-grasp data as in [Ghosh et al. 2023]. \downarrow denotes lower values are better, and \rightarrow denotes values closer to the ground-truth are better. Our results achieves state-of-the-art accuracy across different metrics.

Method	Split		Textual input form		Action correctness	Action correctness over object classes							
	Train split	Test split	Train input	Test input	Overall	apple	mug	train	alarm clock	elephant	medium cylinder	small pyramid	large torus
IMoS*	subject	object	simple	simple	90.3	90.9	89.5	77.8	100	80.0	100	83.3	100
Ours	subject	object	simple	simple	99.5	100	97.4	100	100	100	100	100	100
Ours	object	object	simple	simple	89.7	81.8	92.1	50.0	100	100	100	100	100
Ours	object	object	simple	comprehensive	54.8	40.9	55.3	16.7	52.6	80.0	75	50.0	68.8
Ours	object	object	comprehensive	comprehensive	93.5	95.5	94.7	77.8	100	95.0	93.6	100	93.6

Table 10. **Details of the Text Evaluation.** Comparison of our method against IMoS and our model’s variants that use different forms of textual input. We generate synthetic hand-object pose sequences from each model based on textual prompts in two forms: a simple ("verb" + "object") and our detailed, proposed GRAB dataset annotations ("comprehensive"). We verify whether the generated sequences feature the correct action. We test all methods on our newly created unseen object split, which excludes 7 object classes for testing.

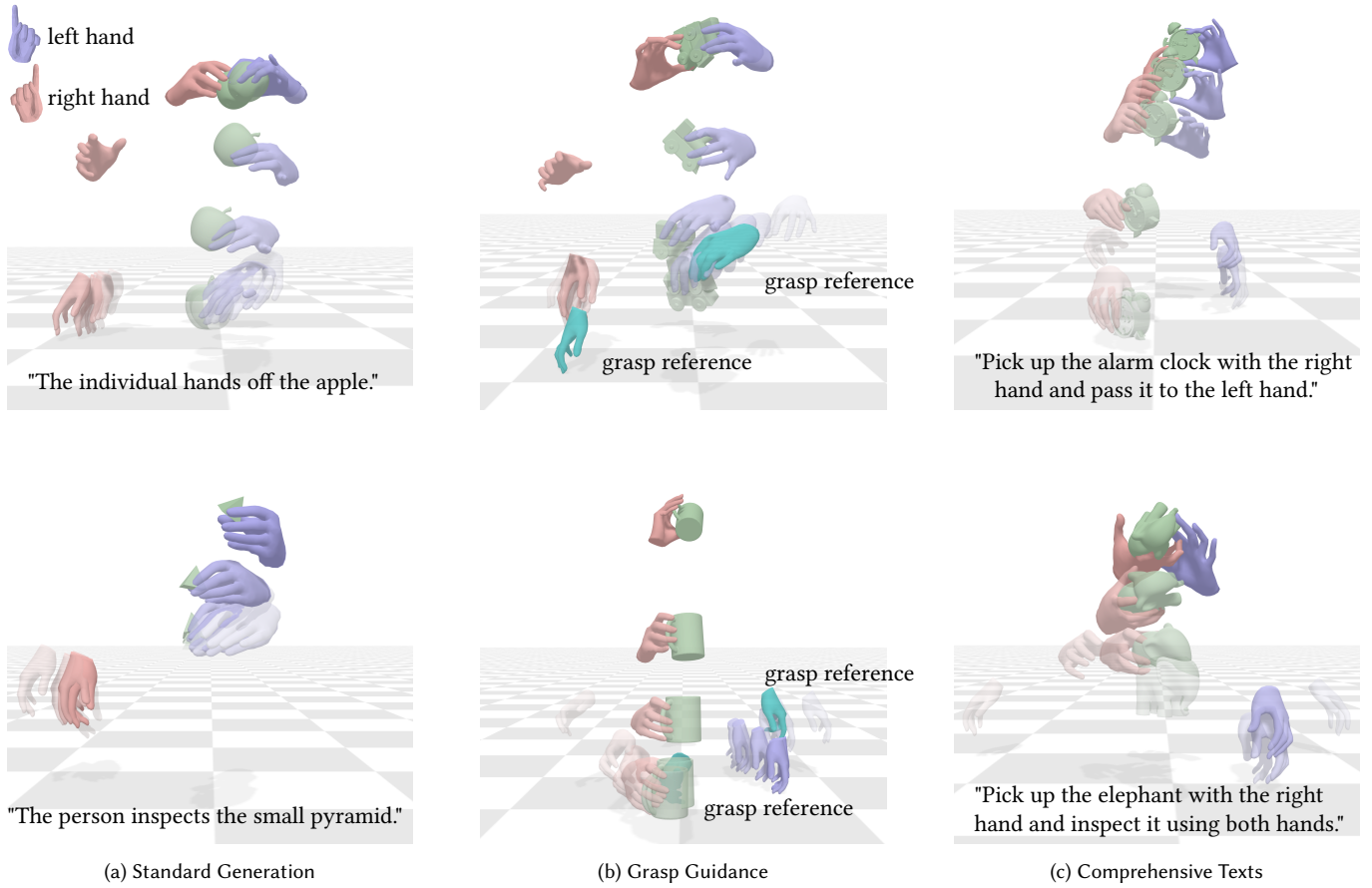


Fig. 6. **Qualitative Examples.** We provide more qualitative examples with a) standard generation without any guidance b) grasp guidance c) our model trained with detailed text descriptions.

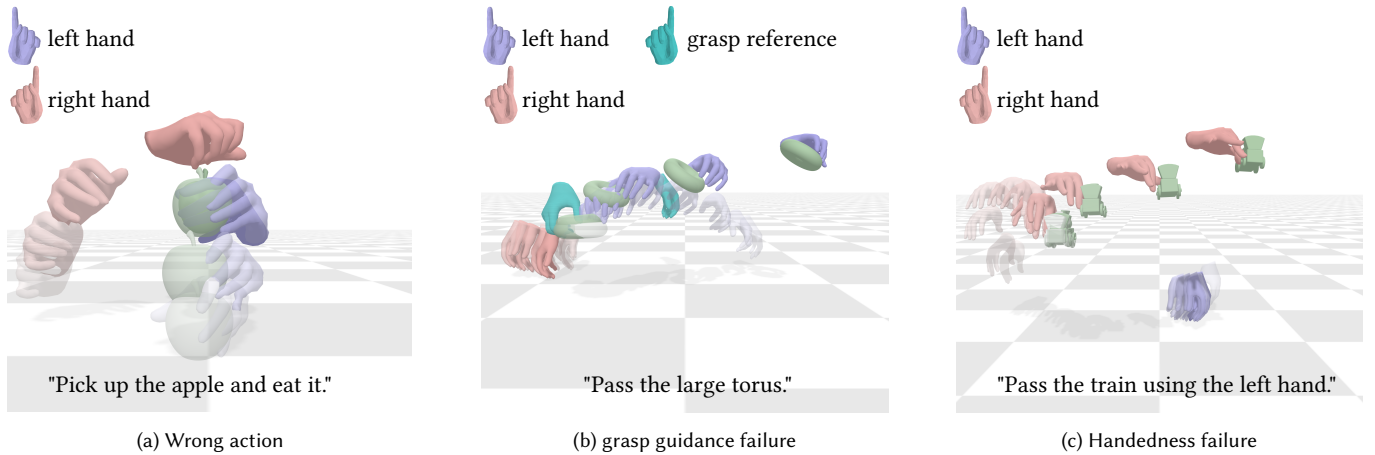


Fig. 7. **Failure Cases.** We present three possible failure cases of our method. a) The generated motion does not match the action described in the input prompt, such as trying to perform a bottle opening motion with an apple. b) During grasp guidance, the reference grasp is largely ignored in the diffusion process, resulting in an interaction that is distinct from the grasp reference. c) Despite training with our curated text annotations, the model sometimes does not pick up on the cue of handedness and may interact with a hand different from the one provided in the text prompt.